RUSSIAN JOURNAL OF EARTH SCIENCES
vol. 20, 3, 2020, doi: 10.2205/2020ES000702

Steric sea-level fluctuations from remote sensing, oceanic reanalyses and objective analyses in the North Atlantic

Aleksey Koldunov[1], *Aleksandr Fedorov*[1], *Igor Bashmachnikov*[1,2], *Tatyana Belonenko*[1]

[1]St. Petersburg State University, St. Petersburg, Russia

[2]Nansen International Environmental and Remote Sensing Centre (NIERSC), St. Petersburg, Russia

Abstract. Five data sets were used to estimate steric level fluctuations in the North Atlantic for 2003-2015. We compare estimates made by a combination of altimetry and GRACE gravity data (ALT-GRV) with assessments obtained from vertical density profiles derived from SODA reanalysis, ARMOR, and EN4 objective analyses. We analyze the datasets without linear trends, and the seasonal signals are also removed. The resulting signals demonstrate the steric sea-level anomalies not related to the linear trends and the seasonal cycles and can be connected with short-period intra-annual variability as well as vortex dynamics of the region since mesoscale eddies can transfer heat and salt and influence thereby the thermohaline water structure from the sea surface to the depth. The deep convection, as well as meandering of the currents also influences the variability of residual time series.

This is the e-book version of the article, published in Russian Journal of Earth Sciences (doi:10.2205/2020ES000702). It is generated from the original source file using LaTeX's **ebook.cls** class.

The steric sea-level fluctuations, obtained from the ARMOR dataset, which incorporates results of satellite observations, shows the best fit for those, derived from ALT-GRV data. The correlation coefficient between ARMOR and ALT-GRV varies between 0.6 and 0.8 over the study region (0.7 on average). Steric sea-level variations derived from SODA or EN4 show good matches with ALT-GRV only for the steric sea-level fluctuations spatially averaged over central regions of the North Atlantic. The discrepancies between the data sets increase northwards and towards the coast. Of the considered data sets, ARMOR is the most suitable for climate studies and research of the sea-level change effects; however, it should be used with caution in the study of the spatial distribution of the steric level.

1. Introduction

Thermal expansion and salinity change of water in the World Ocean cause global changes in sea-level, which are called the steric sea-level fluctuations. An on-going rapid increase in the global air temperature is one of the main indicators and an important driver of the long-

term trends in various parameters of the Earth climate system during the past decades. From 1880 to 2012 the global atmospheric temperature increased by 0.85°C (from 0.65 to 1.06°C, according to different estimates) [*Hartmann et al.,* 2013]. This process also affects the heat content of the World Ocean, manifested as a rise of the global ocean temperature. The global warming affects the steric sea-level, as well as the intensity of its fluctuations. The associated variations in water density do change global sea-level tendencies. Most of the long-term steric sea-level increase comes from ocean warming, but freshening can play a certain role at high latitudes [e.g. *Koldunov et al.,* 2014]. Melting of glaciers and sea-ice reduces ocean salinity, mainly at high latitudes, affecting tendencies in the steric sea-level. *Antonov et al.* [2002] investigated steric sea-level fluctuations of the World Ocean for 1957–1994, using the World Ocean Database. They demonstrated a steady sea-level increase at 50°–65°N with an average rate of about 0.55 mm per year. Steric variations, associated with the decrease in water salinity, account for about 10% of this growth. The authors also found that in the subpolar North Atlantic, an increase in the freshwater flux results in the halosteric anomalies to largely compensate the thermosteric ones. *Levitus et*

al. [2005] examined the contributions of temperature and salinity to the observed linear trends in the steric sea-level height and found that the steric height in the Nordic Seas increases mostly due to the freshening of the upper ocean.

Upper-ocean freshening was also observed in the North Atlantic subpolar gyre of the Labrador-Irminger seas, but due to a compensating cooling, the total variations in the steric height were small in this region. *Curry and Mauritzen* [2005] found a significant increase in the North Atlantic freshwater content during the episode of the Great Salinity Anomaly in the 1970s. The freshening continued at a slower pace until the 1990s when the trend reversed and the freshwater content began to decrease. However, sea-level variations in the North Atlantic can have positive, as well as negative correlations with the steric height. Therefore, altimetry derived sea-level variations in the region are not directly linked to the steric ones. The interpretation of the observations is complicated, also due to the nonlinear nature of the seawater equation of state.

Global sea-level rose by 1.5–2 mm/year over the past century [*Wadhams and Munk,* 2004] and accelerated to 3 mm/year [*Church and White,* 2011]. Recent studies and the latest IPCC special report have

shown that the average sea-level is currently increasing at a speed of about 3.6 mm/year. About 1.40 [from 1.08 to 1.72] mm/year of this trend results from the thermosteric effects (IPCC Special Report on the Ocean and Cryosphere in a Changing Climate, 2019, https://www.ipcc.ch/srocc/downlo ad-report/). The rate of reanalysis data, as well as sea-level change, depends on the region. There is a general similarity between spatial distributions of the trends in the sea-level and those in corresponding steric component [*Fu and Roemmich,* 2018].

The nature of processes contributing to recently observed global-mean steric sea-level changes has not been well understood. *Han et al.* [2016] considered steric sea-level fluctuations in the North-West Atlantic for the period 1993–2012. They used monthly averaged temperature and salinity data for the upper 1500 m of the water column (see for the details of the methodology *Ishii et al.* [2006], *Ishii and Kimoto* [2009]). The derived estimates of the steric sea-level fluctuations were compared with those derived from satellite altimetry. *Han et al.* [2016] showed a link between seasonal and interannual variations of the sea-level and variations in large-scale atmospheric and oceanic processes in the North Atlantic. The steric fluctuations

in the western part of the Labrador Sea are negatively correlated with the North Atlantic Oscillation (NAO). This was attributed to NAO affecting the intensity of winter deep convection in the sea [*Bashmachnikov et al.*, 2018, 2019; *Fedorov et al.*, 2019]. This is due to an increase/decrease of the mean density as a result of intensification/reduction of dense deep water formation during the increase/decrease of the deep convection intensity [*Dickson et al.*, 1996, 2002].

The regional sea-level variations also can be very dynamic. In the central parts of the subpolar gyres, sea-level rise can also result from weakening of the cyclonic circulation [*Belonenko and Fedorov*, 2018; *Belonenko et al.*, 2018; *Hakkinen and Rhines*, 2004, 2009; *Lee et al.*, 2010]. An observed westward shift of Subarctic Front in the eastern part of the Subpolar Gyre [*Belonenko and Fedorov*, 2018; *Belonenko et al.*, 2018; *Bersch*, 2002] can also contribute to the overall sea-level variations in the region.

Assessments of the steric level are highly dependent on the datasets used [*Rhein et al.*, 2013; *Storto et al.*, 2017]. A comparison of 16 ocean reanalyses and 4 objective analyses data for 2003–2010 in the frame of the Ocean Reanalyses Intercomparison Project, highlighted the ARMOR data to be one of the most reliable product

for assessment of steric sea-level variations [*Storto et al.*, 2017]. In this paper, we expand the previous studies and include the SODA reanalysis data as well as EN objective analysis data (EN4) for analysis of the steric sea-level variations. The SODA and EN4 data have not been previously used for the assessment of steric sea-level components. Hence, the comparison of obtained steric sea-level assessment using the SODA reanalysis data and EN objective analysis data to estimations derived by the satellite data have not conducted. In this paper, we use the combination of the satellite data (altimetry and GRACE), the ARMOR data-set, reanalysis SODA, and EN objective analysis for the study of the steric sea-level. Compared to the study by *Storto et al.* [2017], our analysis focuses on the North Atlantic region since it is a key part of the Earth climate system and the Atlantic Meridional Overturning Circulation [see e.g. *Bashmachnikov et al.*, 2018, 2019; *Dickson et al.*, 1996, 2002]. It is important to say that the current research continues the previous studies of the steric sea-level change conducted by the authors. *Belonenko and Koldunov* [2019] have already explored the spatial distribution of linear trends in the North Atlantic using the same data sets. They conclude that the using of altimetry and gravity measurement combina-

tion gives a fundamental opportunity to assess directly the steric level fluctuations in the ocean.

However, there are some geographical limitations in the application of the method due to the elastic deformation of the ocean floor and the corresponding redistribution of water volumes [*Belonenko and Koldunov* [2019; *Frederikse et al.*, 2017; *Kuo et al.*, 2008; *Ray et al.*, 2013]. reveal the greatest bias in trends and errors in determining of the steric sea-level anomalies near Greenland. They also establish the influence of the negative trend component in the GRACE data and conclude that the indicated errors are strongly connected with the GRACE measurements due to modification of the gravitational signal around Greenland. The reason is the melting of ice in Greenland and the corresponding change of the ocean mass. However, the linear trends away from Greenland calculated using the ARMOR data-set, reanalysis SODA, and EN objective analysis consistent with each other and also correlate with the linear trends estimated using the combination of the satellite data, although the spatial distribution of the linear trend coefficients is heterogeneous substantially. There are the large areas (e.g. south to Iceland) with a negative linear trend, where the coefficients reach -10 mm/year, as well as the regions (e.g.

the Labrador sea or the middle latitudes of the North Atlantic) with positive coefficients of the linear trends up to 10 mm/year. There are also large areas with zero trends. It is important to notice that all trends of steric sea-level anomalies show significant similarities in the spatial distribution and their estimates [*Belonenko and Koldunov,* 2019].

The current study extends the previous research by the authors. Hereafter, we analyze the same datasets with removed linear trends and seasonal signals. The resulting signals are connected with a variability of the steric sea-level anomalies not related to the linear trends and the seasonal cycles. These signals can reflect inter-annual variability as well as short-period intra-annual variability, which can be due to e.g. vortex dynamics of the region since mesoscale eddies can transfer heat and salt and influence thereby the thermohaline water structure from the sea surface to the depth. The deep convection, as well as meandering of the currents also influences the variability of residual time series. Thus, we analyze the contribution of residual factors affecting the steric sea-level fluctuations in the North Atlantic after removing linear trends and seasonal factors. This is the main goal of the current analysis where we compare the temporal variability of the steric sea-level anomalies

in the residual signals derived by a combination of the satellite data (altimetry and GRACE) to the anomalies calculated by the ARMOR, SODA, and EN4 data-set. The period under consideration is limited to the span of the GRACE mission – 2003–2010.

2. Data

2.1. Satellite Altimetry

The Ssalto/Duacs altimeter products were produced and distributed by the Copernicus Marine and Environment Monitoring Service (CMEMS) (https://www.copernicus.eu/en/services/marine). We use weakly Sea-level Anomalies (SLA) corrected (instrumental errors, geophysical effects, tidal influence, atmospheric wind and "inverse barometer" effects) data, generated by merging multi-satellite altimetry data, objectively interpolated to a 0.25°Mercator projection grid.

2.2. Ocean Mass From GRACE

Gravity related sea-level anomalies (SLAmass) were obtained from the Gravity Recovery and Climate Experiment (GRACE), processed by Don P. Chambers, sup-

ported by the NASA MEaSUREs Program, and are available at http://grace.jpl.nasa.gov as a $1^\circ \times 1^\circ$ monthly gridded product. Derivation of ocean mass variations from the GRACE gravity observations is described by *Chambers and Bonin* [2012]. The data are available from 2003, which is the reason for such a time limit for the rest of the datasets. Although uncertainties in ocean mass are higher toward northern latitudes, *Chambers and Bonin* [2012] found a good agreement between the GRACE data and in-situ bottom pressure even near the North Pole. The GRACE satellites do not responsive to the sea-level variations induced by local atmospheric pressure changes. However, since water can be considered incompressible, the GRACE data have to be corrected for the globally averaged atmospheric pressure (global inverted barometer correction). We use Level-3 CSR (Center for Space Research at University of Texas) product with the global inverted barometer correction using the monthly mean sea-level pressure from ERA-Interim reanalysis (see [*Dee et al.*, 2011]). The period under consideration is 2003–2015, and it has several data-gaps due to various technical reasons (see for details the official GRACE mission portal (https://podaac.jpl.nasa.gov/GRACE).

2.3. SODA Ocean Reanalysis

SODA (Simple Ocean Data Assimilation) ocean reanalysis (https://www2.atmos.umd.edu/ ocean/) is based on the GFDL MOM5/SIS eddy-permitting ocean model with 0.25°resolution and 50 vertical levels. The model includes the SIS1 active sea ice module, and it is forced by ERA-Interim atmospheric reanalysis. We use monthly the SODA 3.4.2 dataset. Assimilated data include multiple sources: vertical hydrographic profiles of the World Ocean Atlas, ocean moorings, satellite altimetry, sea-surface temperature/salinity in-situ and satellite observations temperature and salinity [*Carton and Giese,* 2008; *Carton et al.,* 2000].

2.4. EN4 Objective Analyses

EN4 dataset (http://hadobs.metoffice.com/en4/download-en4-0-2.html) consists of two products: global quality controlled ocean temperature/salinity profiles and monthly objectively analyzed 3D maps with uncertainty estimate by the Met Office Hadley Centre [*Good et al.,* 2013]. We use the monthly EN4.0.2 dataset. The dataset is based on water temperature/salinity vertical profiles from the World Ocean Data Base, GTSPP, Argo, and ASBO collections. The objectively analyzed

data are distributed at a regular $1^\circ \times 1^\circ$ grid and 42 vertical levels. The backgrounds for the analyses are forecasts of the ocean state generated by persisting anomalies from the previous month.

2.5. Ocean Reanalysis Combining Model and Observations Through an Assimilation Method ARMOR

ARMOR 3D dataset (http://marine.copernicus.eu/services-portfolio/access-to-products/?option= com_csw&view=details&product_id=MULTIOBS_ GLO_PHY_REP_ includes the global 3D temperature/salinity monthly values at 0.25° grid, at standard 50 oceanographic levels [*Verbrugge et al.*, 2017]. This product combines satellite temperature/salinity and sea-level anomalies with in-situ temperature/salinity profiles. Initially, the synthetic vertical profiles are created at a regular grid, using previously obtained multiple regression dependences between satellite temperature/sea-level anomalies and temperature/salinity observations at standard levels. These synthetic profiles are then combined with in-situ and temperature/salinity profiles using optimal interpolation method to form the 3D distributions [*Guinehut et al.*, 2012].

3. Method

3.1. Steric Sea-Level From Satellite Data

Sea-level anomaly (SLA) in the ocean is the sum of two components: $\mathrm{SLA} = \mathrm{SLA}_{\mathrm{mass}} + \mathrm{SLA}_{\mathrm{ster}}$. Here $\mathrm{SLA}_{\mathrm{mass}}$ is the sea-level anomaly associated with variations in the mass of the water column. These changes may occur due to the ocean-atmosphere interaction, the influx of freshwater or melting of ice, etc. $\mathrm{SLA}_{\mathrm{ster}}$ is the level changes due to steric sea-level variations.

Gravimetric measurements from the GRACE satellites allow the evaluation of SLA mass [*Chambers,* 2006]. SLA is corrected for the inverted barometer, tidal and other effects, etc. SLA can estimate the long-term sea-level fluctuations with an accuracy of 2–4 cm [*Fu and Le Traon,* 2006]. Combination of $\mathrm{SLA} = \mathrm{SLA}_{\mathrm{mass}}$ permits a direct assessing of the $\mathrm{SLA}_{\mathrm{ster}}$ fluctuations. This approach is presented in *Chambers* [2006], *Lombard et al.* [2007], *García et al.* [2007], *Storto et al.* [2017]; the application to the Barents Sea is presented in *Volkov et al.* [2013].

The method to calculate the values of the steric sea-level is very easy: $\mathrm{SLA}_{\mathrm{ster}} = \mathrm{SLA} - \mathrm{SLA}_{\mathrm{mass}}$ (altimetry minus gravimetry). When we assess the steric sea-level

using reanalyses or a combination of the satellite data for the 2003–2010 period, we mean the anomalies relative to the zero surface. It is clear to understand for the reanalysis where the zero surfaces are defined by the coordinate system. The zero surface in altimetry is MDT (Mean Dynamic Topography). The altimeter measures the distance between the sea surface and the satellite location. Then, we get SSH which is the height of the sea surface relative to the ellipsoid from the height of the orbit and an ellipsoid model. A useful dynamic characteristic for the oceanographers is the dynamic topography (DT), which defines the currents in the World Ocean:

DT = SSH – geoid.

DT is a sum the Mean Dynamic Topography and sea-level anomalies (SLA):

DT = MDT + SLA.

On the other hand, SLA is the difference between the Sea Surface Height (SSH) and the Mean Sea Surface (MSS):

SLA = SSH – MSS.

Moreover, by definition, MSS = geoid + MDT hence geoid = MSS – MDT and DT = SSH – geoid = SSH – MSS + MDT.

Thus, SLA = SSH – MSS.

SLA is the sea-level anomalies, which include the steric sea-level component as the altimeter measures the distance from satellite, which changes due to water density variations. GRACE also gives sea-level anomalies, on which water density variations do not influence. Notice, the comparison of the altimetry to GRACE anomalies needs to subtract the average values from both rows over the same time interval. When we subtract the second term (GRACE anomalies) from the first one (anomalies from altimetry), we get the steric sea-level anomalies. A combined data set of altimetry and GRACE data in the following is referred to ALT-GRV. Since the altimetry and gravimetric data have different spatial and temporal resolutions initially, we average all data to monthly discreteness and interpolate to a grid with a $1^\circ \times 1^\circ$ spatial resolution using an optimal interpolation algorithm. We exclude the linear trends at each grid-point of the data sets. Then, following *Volkov et al.* [2013], we eliminate the seasonal signal by subtracting the monthly mean climatology from the initial time series. A seasonal climatology is computed as the multiyear monthly average value. By doing so, we remove a large part of the seasonal steric variability that dominates the seasonal variability of SLA. *Belonenko and Fedorov* [2018] also apply

this approach for the Labrador and the Irmiger Seas and demonstrate the strong connection of interannual steric sea-level fluctuations and the intensity of deep convection. Possible spots of the deep convection are shown to be mirrored in spatial distributions of steric sea-level anomalies in the ocean.

3.2. Steric Level From Reanalysis SODA, EN4 and ARMOR Data

Alternatively, steric sea-level can be estimated from vertical temperature-salinity profiles using the integral formula:

$$\mathrm{SLA}_{\mathrm{ster}} = \int_{-1500}^{0} \frac{\rho_0(S_0, T_0, P_0) - \rho(S, T, P)}{\rho_0(S_0, T_0, P_0)} dz$$

where ρ is the density of water, S, T, and P are the monthly mean salinity, temperature, and pressure; S_0, T_0, P_0 are the overall time-mean salinity, temperature, and pressure, respectively [*Kuo,* 2006; *Han et al.,* 2016]. Density ρ is computed from the *UNESCO* [1981] equation of state.

4. Results

An example of spatial distribution of residual steric sea-level anomalies for March and September of 2009 is presented in Figure 1. Note the best match in the spatial distribution is between ALT-GRV and ARMOR. In Figure 1, the overall spatial distribution of SLAster, as well as this at mesoscale, is very similar, despite a large variability of the steric sea-level, in particular in the area of influence of the Gulf Stream and the North Atlantic current. This similarity may be partly due to the way of reconstruction of vertical $T - S$ profiles in ARMOR, where, among other data, sea-level satellite altimetry is used. The SLAster from SODA matches less the results from ALT-GRV data, in particular in what concerns the mesoscale structures. Note EN4 does not resolve mesoscale features, and we can only compare large-scale spatial variability. Both SODA and EN4 quite well reflect large-scale variations of ALT-GRV SLA_{ster}. However, there are also quite strong disagreements in some areas, especially along the coast.

To access whether the observed discrepancies are confined to a particular season or some time interval we determined the correlations between the steric sea-level anomalies fields at each date and revealed the vari-

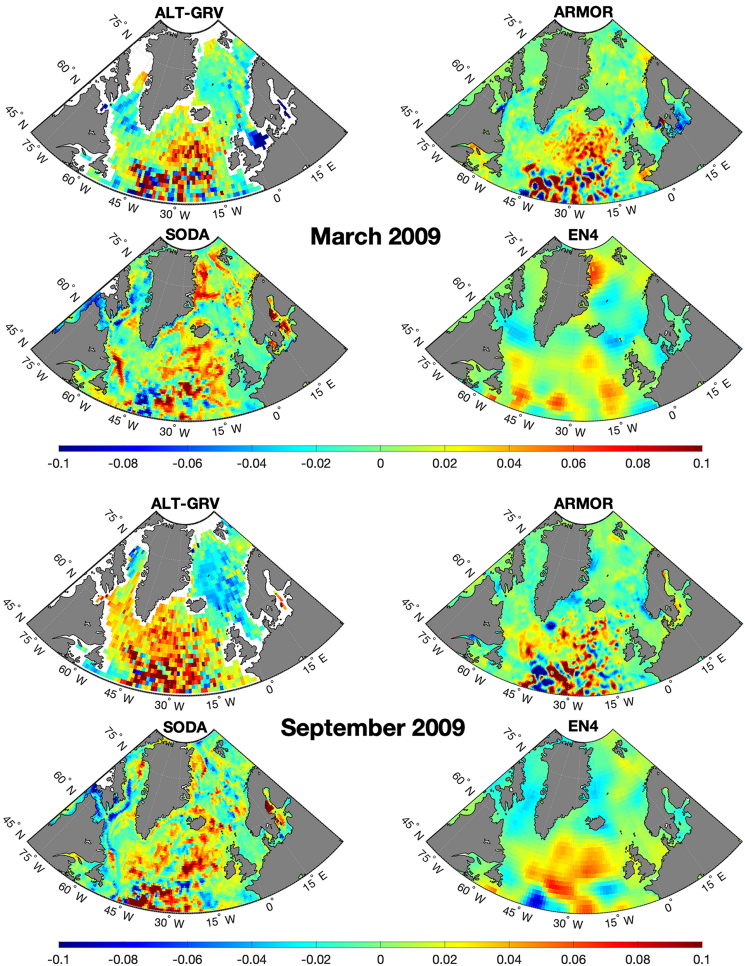

Figure 1. Spatial distribution of the steric sea-level anomaly (m) for the North Atlantic region based on satellite data (ALT-GRV), SODA, EN4, and ARMOR (year 2009). The linear trends and seasonal variability are removed.

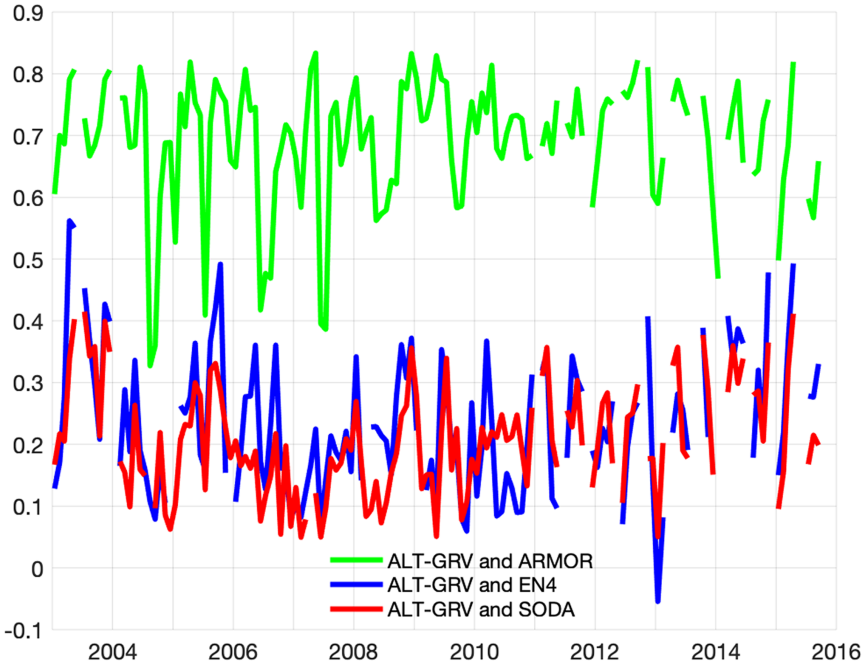

Figure 2. Time series of the correlation coefficients between the steric sea-level anomalies fields. The linear trends and seasonal variability are removed.

ability in time of the correlation coefficient (Figure 2). All data sets preliminarily are interpolated to a satellite data grid ($1/4^\circ \times 1/4^\circ$). Correlation coefficients with a p-level of less than 0.05 are not shown. As expected, ARMOR much better than other datasets represents the ALT-GRV spatial distribution at any time. The

correlation coefficients vary between 0.6 and 0.8 for ARMOR and ALT-GRV, while for SODA and EN4 the correlations vary between 0.1 and 0.3, seldom exceeding 0.4. The time variance of the correlation coefficients between ARMOR and ALT-GRV decreases after 2008, but the variance is likely to increase again after 2013 (although it is difficult to make a definite conclusion due to a large number of gaps in the gravity data). In the case of SODA and EN4, there is no noticeable change in the variance with time. During the latest 6 years of the study period, there is a small increase in the correlation coefficient. The correlation coefficients between all data sets do not demonstrate a seasonal dependence, although for 2003–2010 the correspondence between ARMOR and ALT-GRV is much worse during summer (the correlation decreases to 0.4). Table 1 shows the main statistical parameters when the spatially averaged ARMOR, EN4, and SODA datasets compared to the spatially averaged ALT-GRV data. Notice that the values of the standard deviation of the datasets as well as the root-mean-square errors are very small (they do not exceed 1 cm for ARMOR, EN4, and SODA and a bit more for the ALT-GRV data). Moreover, the values of the bias (systematic errors) are extremely small. Table 1 reveals also the best correlation

Table 1. Variability of Potential Density at Different Depths According to the Aqualog Data for the Cold Season of 2015–2016

Dataset	Standard deviation (m)	Bias (m)	Root-mean-square error (m)	Correlation coefficient
ALT-GRV	0.015	0	0	1.00
ARMOR	0.006	5.725e−05	0.011	0.74
EN4	0.008	−7.615e−05	0.012	0.59
SODA	0.008	6.997e−05	0.011	0.65

of ALT-GRV to ARMOR with the coefficient 0.74 and fewer coefficients for EN4 and SODA.

To determine areas of a better/worse correspondence between datasets, correlation coefficients were time-averaged at each grid point (Figure 3, all data sets are previously interpolated to the ALT-GRV grid). The resulting maps (Figure 3) show that the correspondences between the datasets are highly regionally-dependent. A particularly poor agreement is found in the northern parts of the study region and along the coasts. There is only one region with high correlation coefficients, in which the values of the steric sea-level anomalies agree well for all data sets: the zone south of Greenland, which includes the central Labrador and Irminger seas. The Norwegian Sea is also an area of comparatively good compliance, especially between ALT-GRV and ARMOR.

We use also the Taylor diagram (Figure 4) to quantify the degree of correspondence between the observed data ALT-GRV and ARMOR, EN4, and SODA behavior in terms of three statistics: the Pearson correlation coefficient, the root-mean-square error (RMSE) error, and the standard deviation [*Maze,* 2019; *Taylor,* 2001]. ARMOR, EN4, and SODA, each represented by a different letter on the diagram, are compared, and the dis-

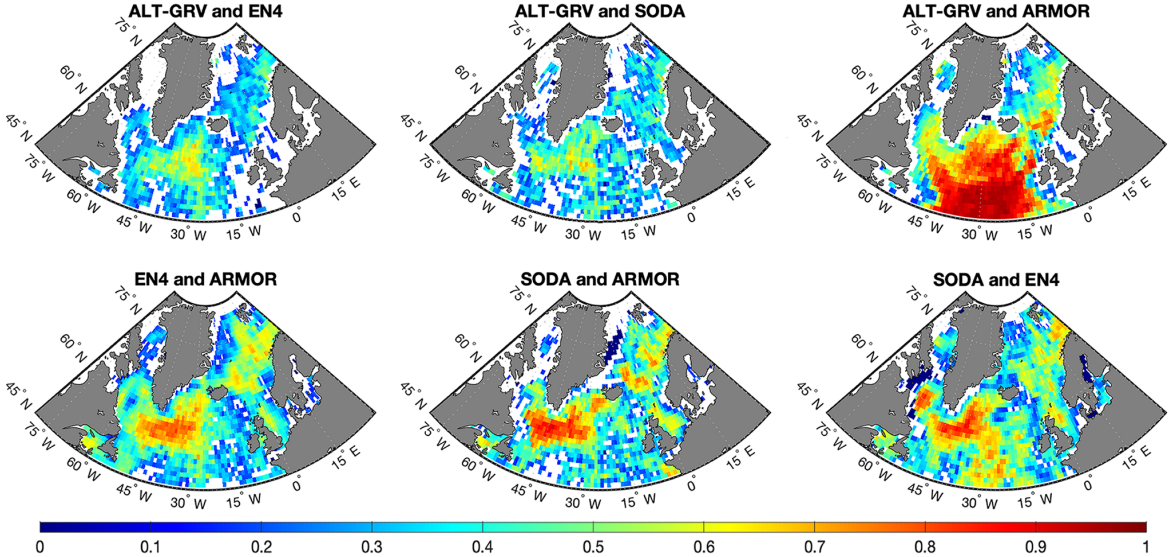

Figure 3. Spatial distribution of the correlation coefficients between the data sets. The linear trends and seasonal variability are removed.

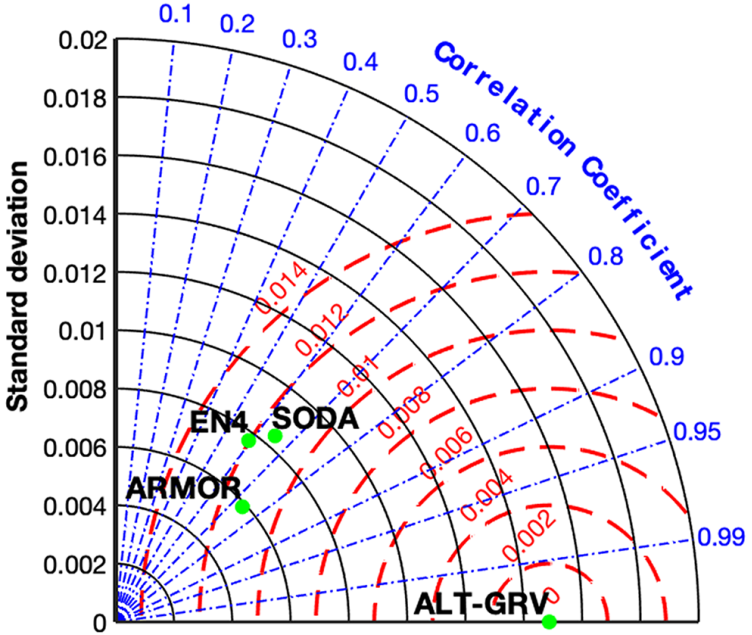

Figure 4. Taylor diagram displaying a statistical comparison with observations of the spatially averaged ALT-GRV, ARMOR, EN4, and SODA datasets for the study area.

tance between them and the point labeled "ALT-GRV" is a measure of how realistically each model reproduces observations. For each model, three statistics are plotted: the Pearson correlation coefficient is related to the azimuthal angle (blue contours). The centered RMS error in the simulated field is proportional to the distance from the point on the x-axis identified as "ALT-GRV"

(green contours), and the standard deviation of the simulated pattern is proportional to the radial distance from the origin (black contours). It is evident from this diagram, for example, that for ARMOR the correlation coefficient is about 0.74, the RMS error is about 0.011 m and the standard deviation is about 0.006 m.

Averaged over the study area, the time series of steric sea-level anomalies, derived from temperature-salinity profiles correlate reasonably well with those of ALT-GRV (Figure 5). The correlation coefficients range from 0.6 for EN4 to 0.7 for ARMOR. Area-mean steric sea-level fluctuations from ARMOR, EN4, and SODA also highly correlated with each other, with correlation coefficients 0.83–0.88. However, the result strongly depends on the region, over which the data are averaged (see Figure 3). Figure 5 also displays the values of the intra-annual correlation coefficients, which are calculated by excluding all inter-annual variability from the time series (the graphs of the excluded inter-annual time series are not shown but only the values of the correlation). The correlation of intra-annual variability is 0.61 only for EN4 and SODA, and it is very small for the datasets (Figure 5).

We have identified two areas in which there is a maximum correspondence between all the datasets under

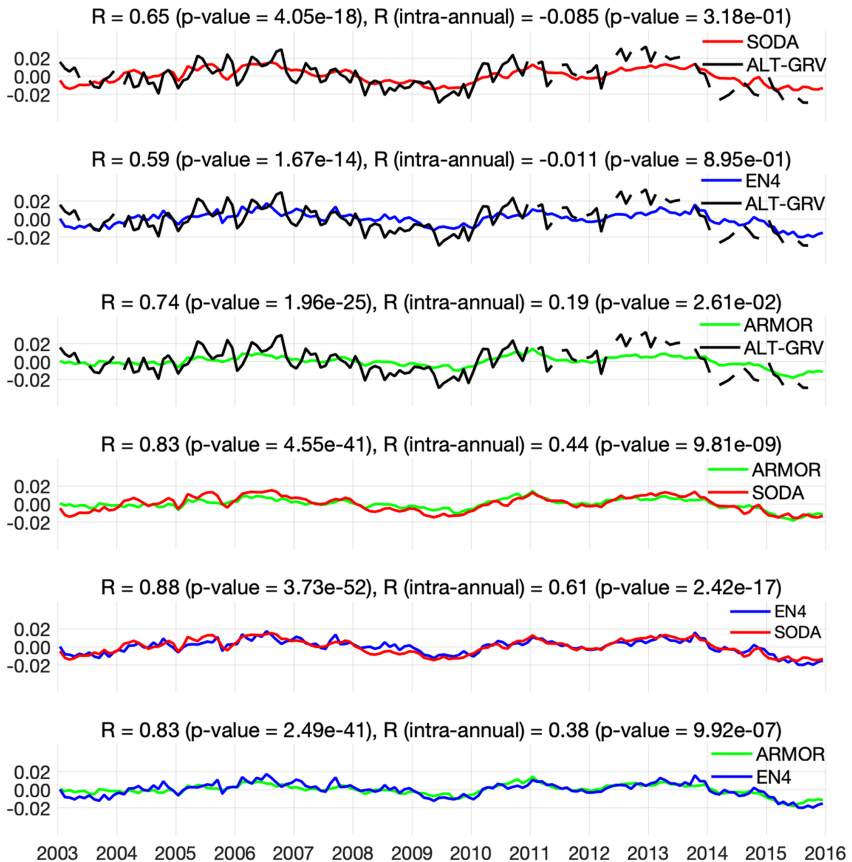

Figure 5. Time series of the steric sea-level fluctuations (m) averaged over the study region, R is the correlation coefficient, R (intra-annual) is calculated by the time series excluding all inter-annual variability, p-value is the probability of obtaining the observed results of a test, assuming that the null hypothesis is correct). The linear trends and seasonal variability are removed.

consideration. Region A, which includes the Labrador and the Irminger seas, and region B, comprising the Norwegian Sea (Figure 6). The Taylor diagrams of the SODA, EN4, and ARMOR datasets compared to ALT-GRV for areas A and B are shown in (Figure 7). Figure 8. shows the time series of steric sea-level fluctuations for the two selected regions in Figure 6. As before, ARMOR shows the best correspondence with ALT-GRV. The correlation is 0.8 for region A. However, now there is no such big difference with the rest of the data sets. For example, the correlation coefficient of EN4 with ALT-GRV is 0.7. A good fit is, correspondingly, derived between the SODA, EN4, and ARMOR datasets (the correlation coefficient is about 0.9). For region B, the difference between the correlated pairs is even smaller and the correlation coefficients are almost the same, although lower (about 0.6). Notice, that the intra-annual correlation coefficients in Figure 8 are bigger than in Figure 5 for the whole region. It might be due to the intra-annual mesoscale variability of thermohaline processes in the two regions are different.

Thus, we have analyzed the spatial and temporal variability of residual sea-level anomalies in the North Atlantic. Figure 1, Figure 3 and Figure 6 demonstrate that it is spatially heterogeneous. Figure 2, Figure 5

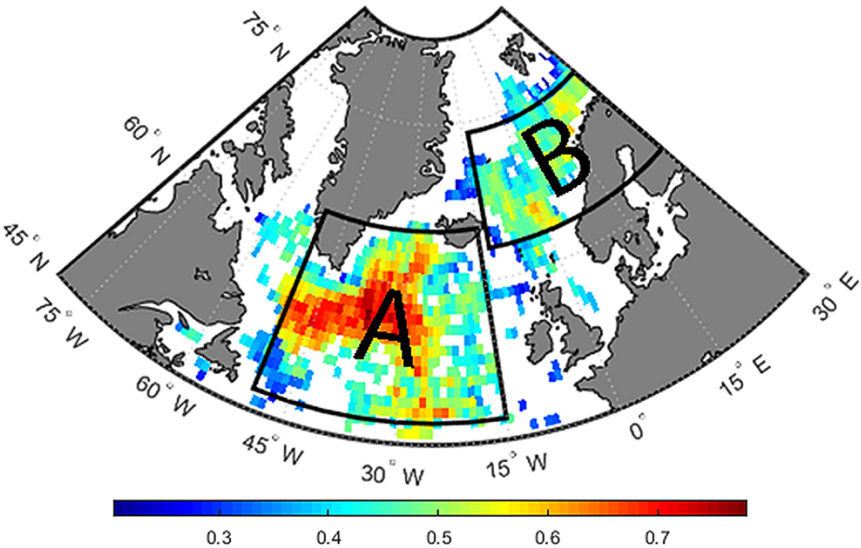

Figure 6. Area boundaries and the distribution (color) of the mean of the correlation coefficients between all datasets. The linear trends and seasonal variability are removed.

and Figure 8 show the temporal variability, which is essentially non-stationary. Figure 9 presents squared wavelet coherence [*Grinsted,* 2004] between the spatially averaged datasets time series. It reveals maxima for a 2–3-year period corresponding to the most stable connection of datasets from 2008–2009. Thus, the inter-annual variability of the 2–3-year period is characteristic only for the second half of the rows. The max-

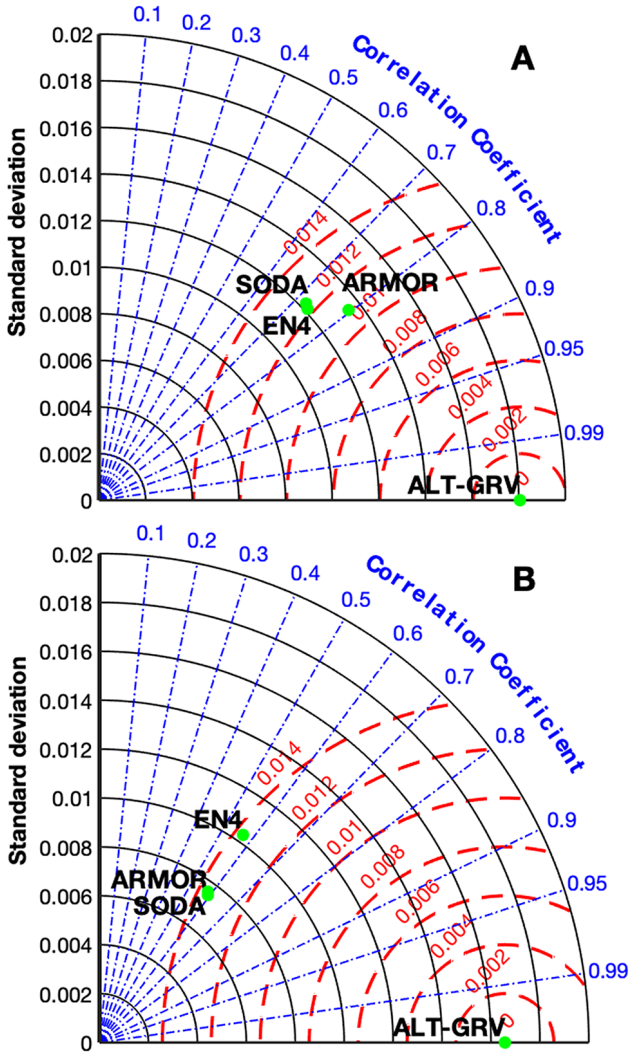

Figure 7. Taylor diagram displaying a statistical comparison with observations of the spatially averaged ALT-GRV, ARMOR, EN4, and SODA datasets for the area A and B.

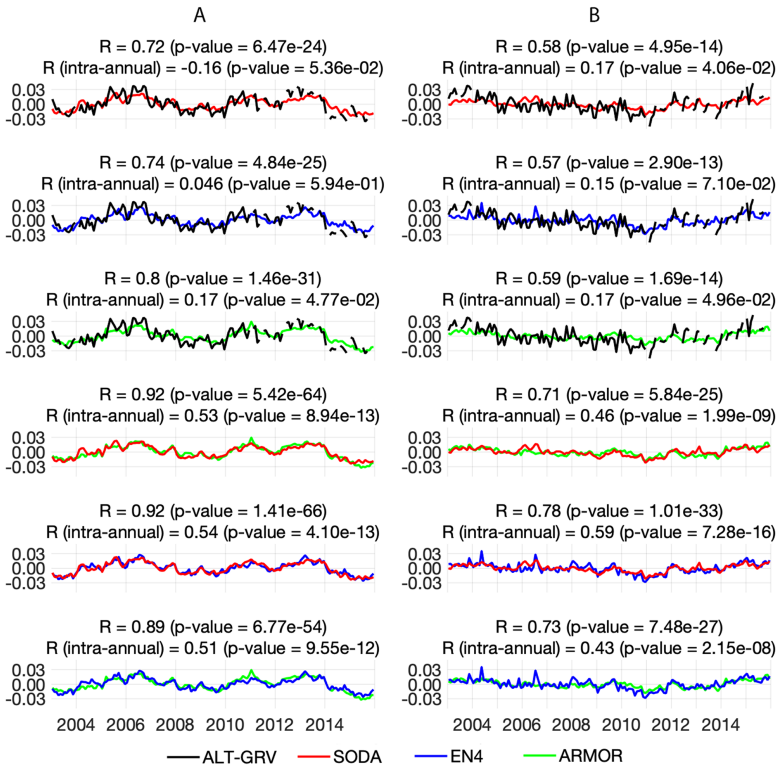

Figure 8. Time series of the steric sea-level fluctuations (m) averaged over area A (left column) and area B (right column). The linear trends and seasonal variability are removed.

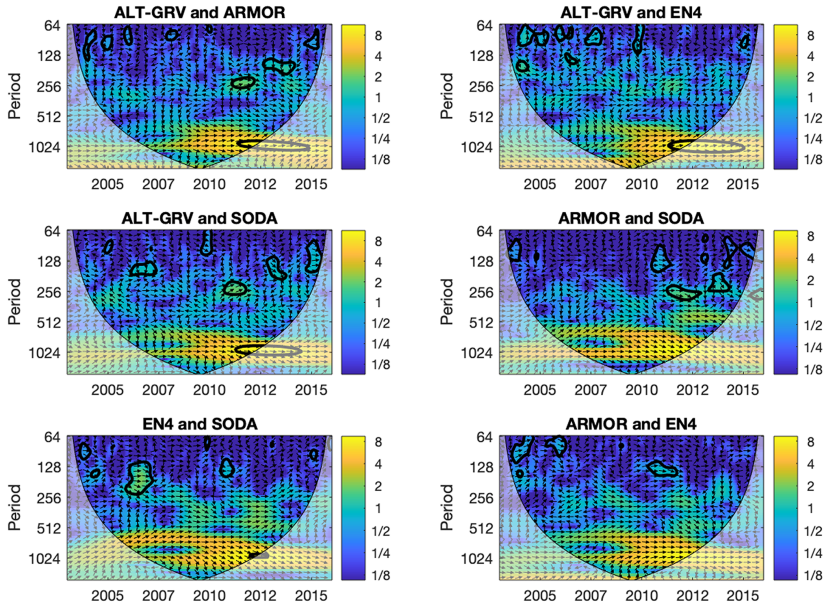

Figure 9. Squared wavelet coherence between the spatially averaged datasets time series (averaging for the study area). The 5% significance level against red noise is shown as a thick contour. The relative phase relationship is shown as arrows (with in-phase pointing right, anti-phase pointing left), and the arrows represent the complex arguments of the wavelet power.

ima for the 2–3-year period from 2008–2009 can be due to ocean-atmosphere interaction because of the quasi-biennial oscillation in the Earth's atmosphere [*Khairullina and Astafieva,* 2011]. Another explanation can be connected with deep convection in the North Atlantic,

which is observed after 2008 [*Belonenko and Fedorov,* 2018]. However, both of them are just a hypothesis. On the contrary, the intra-annual changes are revealed mostly at first of the rows. However, the values of the coherence of them are significantly less.

5. Conclusions

Five datasets were used to estimate steric sea-level fluctuations in the North Atlantic for the period 2003–2015. For the satellite datasets, the difference between altimetry measurements and GRACE bottom pressure (ALT-GRV) has been transformed into the steric sea-level anomalies. The vertical density profiles from EN4 objective analyses, SODA reanalysis, and ARMOR satellite and in-situ data were transformed into steric sea-level variations. We compare the datasets: ALT-GRV, EN4, SODA, and ARMOR after removing linear trends and seasonal signals. The residual datasets reflect the spatial and temporal variability of mesoscale features in the North Atlantic. They are affected by the vortex dynamics of the region since mesoscale eddies can transfer heat and salt and influence thereby the thermohaline water structure from the sea surface to the depth. The other reasons are mesoscale meandering

the currents, deep convection and any other kind processes of short-period intra-annual variability changing the water properties. Similar to *Storto et al.* [2017], we found that ARMOR is the best for estimating the spatial and temporal variations of the steric sea-level anomalies. SODA and EN4 gave significantly worse results when comparing the spatial distribution of the steric fluctuations, but the results are comparable to ARMOR results when accessing temporal evolution of the fluctuations, averaged over large areas of the study region. That compliance is highly area-dependent. The best fit of the time fluctuations to the satellite data was obtained for the central Labrador and Irminger seas. Relatively high correlations were also obtained for the central Norwegian Sea. In the northern part of the study region and the coastal areas, correlations of time fluctuations of the steric sea-level with ALT-GRV do not satisfy the p-level criterion. The wavelet coherence diagrams demonstrate the strong quasi-biennial oscillation of the datasets from 2008–2009 and a bit weaker intra-annual variability from 2003–2008.

Acknowledgments. The authors acknowledge the support of the Russian Science Foundation (RSF, project No. 18-17-00027).

References

Antonov, J. I., S. Levitus, T. P. Boyer (2002) , Steric sea-level variations during 1957–1994: Importance of salinity, *J. Geophys. Res.*, *107*, no. C12, p. 8013, **Crossref**

Bashmachnikov, I. L., A. M. Fedorov, A. V. Vesman, et al. (2018) , Thermohaline convection in the subpolar seas of the North Atlantic from satellite and in situ observations. Part 1: Localization of the deep convection sites, *Sovremennye Problemy Distantsionnogo Zondirovaniya Zemli iz Kosmosa*, *15*, no. 7, p. 184–194, **Crossref**

Bashmachnikov, I. L., A. M. Fedorov, A. V. Vesman (2019) , Thermohaline convection in the subpolar seas of the North Atlantic from satellite and in situ observations. Part 2: Indices of intensity of deep convection, *Sovremennye Problemy Distantsionnogo Zondirovaniya Zemli iz Kosmosa*, *16*, no. 1, p. 191–201, **Crossref**

Belonenko, T. V., A. V. Koldunov (2019) , Trends of Steric Sea-level Oscillations in the North Atlantic, *Izvestiya, Atmospheric and Oceanic Physics*, *55*, no. 9, p. 1106–1113, **Crossref**

Belonenko, T. V., A. M. Fedorov (2018) , Steric Level Fluctuations and Deep Convection in the Labrador and Irminger Seas, *Izvestiya, Atmospheric and Oceanic Physics*, *54*, no. 9, p. 1039–1049, **Crossref**

Belonenko, T. V., A. M. Fedorov, I. L. Bashmachnikov, et al. (2018) , Current Intensity Trends in the Labrador and Irminger Seas Based on Satellite Altimetry Data, *Izvestiya, Atmospheric and Oceanic Physics*, *54*, no. 9, p. 1031–1038, **Crossref**

Bersch, M. (2002) , North Atlantic Oscillation – induced changes

of the upper layer circulation in the northern North Atlantic Ocean, *J. Geophys. Res.*, *107*, no. C10, p. 3156, **Crossref**

Carton, J. A., G. Chepurin, X. Cao, et al. (2000) , A Simple Ocean Data Assimilation analysis of the global upper ocean 1950–1995, Part 1: methodology, *J. Phys. Oceanogr.*, *30*, p. 294–309, **Crossref**

Carton, J. A., B. S. Giese (2008) , A Reanalysis of Ocean Climate Using Simple Ocean Data Assimilation (SODA), *Monthly Weather Review*, *136*, no. 8, p. 2999, **Crossref**

Chambers, D. P. (2006) , Observing seasonal steric sea-level variations with GRACE and satellite altimetry, *J. Geophys. Res.*, *111*, p. C03010, **Crossref**

Chambers, D. P., J. A. Bonin (2012) , Evaluation of Release-05 GRACE time-variable gravity coefficients over the ocean, *Ocean Sci.*, *8*, p. 859–868, **Crossref**

Church, J. A., N. J. White (2011) , Sea-level rise from the late 19th to the early 21st century, *Surveys in Geophysics*, *32*, no. 4–5, p. 585–602, **Crossref**

Curry, R. G., C. Mauritzen (2005) , Dilution of the northern North Atlantic Ocean in recent decades, *Science*, *308*, p. 1772–1774, **Crossref**

Dee, D. P., et al. (2011) , The ERA-Interim reanalysis: configuration and performance of the data assimilation system, *Quarterly Journal of the Royal Meteorological Society, John Wiley [ampersand] Sons, Ltd.*, *137*, p. 553–597.

Dickson, R. R., J. Lazier, J. Meincke, et al. (1996) , Long-term coordinated changes in the convective activity of the North At-

lantic, *Prog. Oceanogr.*, *38*, p. 241–295, **Crossref**

Dickson, R., I. Yashayev, J. Meincke, et al. (2002) , Rapid freshening of the deep North Atlantic Ocean over the past four decades, *Nature*, *416*, p. 832–837, **Crossref**

Fedorov, A. M., I. L. Bashmachnikov, T. V. Belonenko (2019) , Winter convection in the Lofoten Basin according to ARGO buoys and hydrodynamic modeling, *Vestn S. Petersbur. Un-ta, Earth sciences*, *64*, no. 3, p. 491–511, **Crossref**

Frederikse, T., R. E. M. Riva, M. A. King (2017) , Ocean bottom deformation due to present-day mass redistribution and its impact on sea-level observations, *Geoph. Res. Lett.*, *44*, **Crossref**

Fu, L.-L., P.-Y. Le Traon (2006) , Satellite altimetry and ocean dynamics, *Comptes Rendus Geosciences*, *338*, no. 14–15, p. 1063–1076, **Crossref**

Fu, L.-L, D. H. Roemmich (2018) , Monitoring global sea-level change from spaceborne and in situ observing systems, *Bridge*, *48*, p. 54–63.

García, D., G. Ramillien, A. Lombard (2007) , Cazenave Steric Sea-level Variations Inferred from Combined Topex/Poseidon Altimetry and GRACE Gravimetry, *Pure [ampersand] Applied Geophysics*, *164*, no. 4, p. 721–731, **Crossref**

Good, S. A., M. J. Martin, N. A. Rayner (2013) , EN4: quality controlled ocean temperature and salinity profiles and monthly objective analyses with uncertainty estimates, *Journ. of Geoph. Res.: Oceans*, *118*, p. 6704–6716, **Crossref**

Grinsted, A., J. C. Moore, S. Jevrejeva (2004) , Application of the cross wavelet transform and wavelet coherence to geophysical time series, *Nonlin. Process. Geophys.*, *11*, p. 561–566, **Cross-**

ref

Guinehut, S., A.-L. Dhomps, et al. (2012) , High resolution 3D temperature and salinity fields derived from in situ and satellite observations, *Ocean Sci.*, *8*, p. 845–857, **Crossref**

Hakkinen, S., P. B. Rhines (2004) , Decline of subpolar North Atlantic circulation during the 1990s, *Science*, *309*, p. 555–559, **Crossref**

Hakkinen, S., P. B. Rhines (2009) , Shifting surface currents of the northern North Atlantic Ocean, *J. Geophys. Res.: Oceans*, *114*, p. C04005, **Crossref**

Han, G., N. Chen, C. Y. Kuo, et al. (2016) , Interannual and Decadal Sea Surface Height Variability Over the Northwest Atlantic Slope, *IEEE Journal of Selected Topics in Applied Earth Observations and Remote Sensing*, **Crossref**

Hartmann, D. L., A. M. G. Klein Tank, M. Rusticucci, et al. (2013) , Observations: Atmosphere and Surface, *Climate Change 2013: The Physical Science Basis. Contribution of Working Group I to the Fifth Assessment Report of the Intergovernmental Panel on Climate Change (Stocker, T. F., D. Qin, G.-K. Plattner, M. Tignor, S. K. Allen, J. Boschung, A. Nauels, Y. Xia, V. Bex and P. M. Midgley (eds.))*, p. 159–254, Cambridge University Press, Cambridge, United Kingdom, and New York, NY, USA.

Ishii, M., M. Kimoto (2009) , Reevaluation of historical ocean heat content variations with time-varying XBT and MBT depth bias corrections, *J. Oceanogr.*, *65*, p. 287–299, **Crossref**

Ishii, M., M. Kimoto, K. Sakamoto (2006) , Steric sea-level changes estimated from historical ocean subsurface temperature and

salinity analyses, *J. Ocean.*, *62*, p. 155–170, **Crossref**

Khairullina, G. R., N. M. Astafieva (2011) , *Quasi-Beinnial Oscillation in the Earth's Atmophere, Review: Observations and Physical Mechanisms*, 60 pp., IKI RAS, Moscow (in Russian).

Koldunov, N. V., N. Serra, A. Kohl (2014) , Multimodel simulations of Arctic Ocean sea surface height variability in the period 1970–2009, *Journ. of Geoph. Res.: Oceans*, *119*, no. 12, p. 8936–8954, **Crossref**

Kuo, C. (2006) , Determination and Characterization of 20th Century Global Sea Level Rise, Report 478, Ohio State University, Division of Geodetic Science, Columbus, OH, USA.

Kuo, C.-Y., C. K. Shum, J. Guo, et al. (2008) , Southern Ocean mass variation studies using GRACE and satellite altimetry, *Earth, Planets and Space*, *60*, no. 5, p. 477–485, **Crossref**

Lee, T., S. Hakkinen, K. Kelly, et al. (2010) , Satellite observations of ocean circulation changes associated with climate variability, *Oceanography*, *23*, no. 4, p. 70–81, **Crossref**

Levitus, S., J. I. Antonov, et al. (2005) , Linear trends of zonally averaged thermosteric, halosteric, and total steric sea-level for individual ocean basins and the World Ocean, (1955–1959)–(1994–1998), *Geophys. Res. Lett.*, *32*, p. L16601, **Crossref**

Lombard, A., D. Garcia, G. Ramillien, et al. (2007) , Estimation of steric sea-level variations from combined GRACE and Jason-1 data, *Earth Planet Sci Lett.*, *254*, p. 194–202, **Crossref**

Maze, G. (2019), Taylor Diagram, MATLAB Central File Exchange. (https://www.mathworks.com/matlab central/fileexchange/20559-taylor-diagram, Retrieved December 17)

Ray, R. D., S. B. Luthcke, T. van Dam (2013) , Monthly crustal

loading corrections for satellite altimetry, *Journ. of Atmospheric and Oceanic Technology*, *30*, no. 5, p. 999–1005, **Crossref**

Rhein, M., S. R. Rintoul, S. Aoki, et al. (2013) , Observations: Ocean, *Climate Change 2013: The Physical Science Basis. Contribution of Working Group I to the Fifth Assessment Report of the Intergovernmental Panel on Climate Change, Stocker T. F., et al. (eds.)*, p. 255–315, Cambridge University Press, Cambridge, United Kingdom, and New York, NY, USA.

Storto, A., S. Masina, M. Balmaseda (2017) , Steric sea-level variability (1993–2010) in an ensemble of ocean reanalyses and objective analyses, *Climate Dynamics*, *49*, no. 3, p. 709–729, **Crossref**

Taylor, K. (2001) , Summarizing multiple aspects of model performance in a single diagram, *Journ. of Geoph. Res.-Atmospheres*, *V106*, no. D7, p. 7183–7192, **Crossref**

UNESCO, (1981) , Tenth report of the joint panel in ocean graphic tables and standards, *UNESCO Technical Papers in Marine Science, 36*, p. 25, UNESCO, Paris.

Verbrugge, N., S. Mulet, S. Guinehut (2017) , ARMOR3D: A 3D multi-observations T, S, U, V product of the ocean, *Geophys. Res. Abstracts*, *19*, p. EGU2017-17579.

Volkov, D. L., F. W. Landerer, S. A. Kirillov (2013) , The genesis of sea-level variability in the Barents Sea, *Continental Shelf Res.*, *66*, p. 92–104, **Crossref**

Wadhams, P., W. Munk (2004) , Ocean freshening, sea-level rising, sea ice melting, *Geophys. Res. Lett.*, *31*, p. L11311, **Crossref**